

Trends in magnetism of free Rh clusters via relativistic ab-initio calculations

O. Šipr,^{1,*} H. Ebert,² and J. Minár^{2,3}

¹*Institute of Physics of the ASCR v. v. i., Cukrovarnická 10, CZ-162 53 Prague, Czech Republic*

²*Universität München, Department Chemie, Butenandtstr. 5-13, D-81377 München, Germany*

³*New Technologies Research Centre, University of West Bohemia, Pilsen, Czech Republic*

A fully relativistic *ab-initio* study on free Rh clusters of 13–135 atoms is performed to identify general trends concerning their magnetism and to check whether concepts which proved to be useful in interpreting magnetism of 3d metals are applicable to magnetism of 4d systems. We found that there is no systematic relation between local magnetic moments and coordination numbers. On the other hand, the Stoner model appears well-suited both as a criterion for the onset of magnetism and as a guide for the dependence of local magnetic moments on the site-resolved density of states at the Fermi level. Large orbital magnetic moments antiparallel to spin magnetic moments were found for some sites. The intra-atomic magnetic dipole T_z term can be quite large at certain sites but as a whole it is unlikely to affect the interpretation of x-ray magnetic circular dichroism experiments based on the sum rules.

PACS numbers: 75.75.Lf, 75.10.Lp, 78.70.Dm, 75.30.Gw

Keywords: clusters, magnetism, Stoner criterion, anisotropy

I. INTRODUCTION

Magnetism of systems with reduced dimensions is a vivid research area both because of fundamental interest and because of technological relevance. To be able to design new devices based on magnetism of clusters and thin films one should have an intuitive understanding for these, so that one can estimate beforehand which configurations and compositions might be perspective or not. Magnetism of Rh carries a special appeal because it concerns a material which is magnetic only in reduced dimensions and in which the spin orbit coupling (SOC) is expected to play a more important role than in the magnetism of 3d elements. Indeed, Rh magnetism seems to be quite intriguing, with results obtained so far being often controversial and not easy to interpret. Catalytic properties of Rh add yet another impetus for studying low-dimensional Rh systems.

The interest in free Rh clusters was stimulated by a Stern-Gerlach-type experiment on clusters of 9–100 atoms,¹ where it was found that Rh clusters have magnetic moments which decrease with cluster size down from $0.8 \mu_B$ in a non-monotonous way and become strongly suppressed (possibly to zero) for clusters of more than 60 atoms. Another experimental input comes from x-ray magnetic circular dichroism (XMCD) measurements of Sessi *et al.*² who studied quasi-free Rh clusters of few tens of atoms in a Xe matrix on Ag(100) and found that the clusters are magnetic, with an effective spin magnetic moment μ_{spin} of about $0.26 \mu_B$ and with the ratio between orbital and spin magnetic moments $\mu_{\text{orb}}/\mu_{\text{spin}}$ about 40%. Recently, spin and orbital moments induced in paramagnetic Rh clusters of about 220 atoms embedded in a Al_2O_3 matrix were determined also via XMCD³ and it was found that the orbital moment μ_{orb} does not exceed 2% of μ_{spin} .

For a deeper understanding of the magnetism of free Rh clusters and of Rh magnetism in general it would be

useful to identify general trends which Rh-based systems obey. This could be achieved by monitoring the trends for a large set of related systems and comparing them with the situation for (much better studied) 3d elements. Such a study should be performed in a relativistic way because only then possible effects of SOC can be properly included. Also, experiments pose some questions that call for fully relativistic calculations — such as the above mentioned issue of small μ_{orb} measured by XMCD for a set of paramagnetic clusters embedded in Al_2O_3 (Ref. 3) in contrast to large μ_{orb} measured for ferromagnetic clusters in a Xe matrix.²

A considerable effort was devoted to theoretical research on free Rh clusters recently. Even though interesting and important results were obtained, only few systematic studies for large sets of systems were done so only an incomplete picture could have been gathered. This is even more true concerning relativistic properties such as orbital magnetism. Most *ab initio* studies focused on clusters of less than 20 atoms and specifically on their geometries. It turns out that small clusters often tend to have non-compact shapes.^{4–6} The situation is still not clear because different density functional theory (DFT) implementations predict different structures and spin configurations.⁷ Pseudopotential calculations seem to give rise to more open structures than all-electron calculations.⁸ Structural studies for large clusters were performed only within a model *d*-band tight-binding (TB) Hamiltonian and it was found that the relaxation of bond distances for fcc clusters of 13–165 atoms is non-uniform, with some distances decreasing and some distances increasing.⁹

It emerges that the existence of more competing configurations is typical for Rh clusters and sometimes the configurations differ only little in energies but considerably in magnetic moments.^{10–13} It seems that a similar situation arises regarding the suppression of magnetism for large clusters, which occurs for sizes between 60 and 100

atoms according to the experiment.¹ E.g., model Hamiltonian calculations found that for fcc clusters of 55 and 79 atoms magnetic solutions exist but are higher in energy than non-magnetic solutions.⁹ For clusters of 135 and 165 atoms, no magnetic solutions were found.⁹ Pseudopotential calculations for icosahedral clusters yield a finite moment for a 55-atoms cluster and a zero moment for a 147-atoms cluster.¹² At the same time, in order to explain their XMCD experiments, Barthem *et al.*³ suggest that the Stoner criterion may be locally fulfilled at only some atoms in large Rh clusters, giving rise to an inhomogeneous magnetic state.

Connected with the question of size-dependence of magnetic moments is the question of the dependence of local magnetic moments on the coordination numbers. For $3d$ clusters (both free¹⁴ and supported)^{15–17} a distinct relation could be identified in this respect. However, this need not be transferable to $4d$ clusters and there are some hints that a relation of this kind may be absent in Rh systems.^{4,6,18} However, no systematic study about this has been performed so far.

The issue of orbital moments has not yet attracted much theoretical attention. Model d -band TB Hamiltonian calculations were performed for few Rh clusters of up to 27 atoms.^{19,20} It was found that μ_{orb} is typically 10–20% of μ_{spin} . The orbital moment μ_{orb} is nearly always parallel to μ_{spin} and when it is antiparallel to μ_{spin} , it is very small. *Ab initio* calculations performed for Rh clusters of 2–7 atoms lead to similar conclusions: spin and orbital magnetic moments are always parallel to each other and the $\mu_{\text{orb}}/\mu_{\text{spin}}$ ratio is about 10%, except for the smallest clusters.²¹ In all these studies the SOC was added in a second variation approach. However, the SOC may play a more important role in $4d$ clusters and it is not clear whether it can be fully accounted for in this way. Recalling also that recent XMCD studies led to opposite conclusions regarding the $\mu_{\text{orb}}/\mu_{\text{spin}}$ ratio,^{2,3} a more detailed study of orbital magnetism of Rh clusters is desirable.

Concerning the interpretation of experiments, let us mention finally that the XMCD sum rules do not provide a “bare” spin moment μ_{spin} but only its combination with the magnetic dipole T_z term, $\mu_{\text{spin}} + 7T_z$. It is conceivable that a disagreement between theory and experiment may arise partly due to the effect of the T_z term.³ Earlier calculations for Rh₁₉ and Rh₄₃ clusters suggest that this influence should not be crucial for free clusters² but this ought to be analyzed more deeply and for a large set of systems.

It turns out that despite the intense attention that has been devoted to theoretical research on free Rh clusters, some important issues remain to be solved. One of them is whether there is any systematic relation between local magnetic moments and coordination numbers as in $3d$ clusters or whether such a relation is totally absent. Linked to this is a question whether the Stoner criterion can be applied locally, i.e., whether it could be used to estimate local magnetic moments in large clusters. The

relatively large SOC implies a question to what extent will scalar-relativistic results differ from fully-relativistic results. How important is orbital magnetism in Rh clusters, especially in large ones? Is it possible to reconcile large $\mu_{\text{orb}}/\mu_{\text{spin}}$ ratios obtained via XMCD by Sessi *et al.*² with small $\mu_{\text{orb}}/\mu_{\text{spin}}$ ratios obtained by Barthem *et al.*?³ What is the role of the magnetic dipole term T_z ? Could it possibly be responsible for the deviations between some theories and XMCD experiments?

To address these issues, we performed a fully-relativistic theoretical study of clusters of 13–135 atoms and also of free-standing monolayers (for comparison). We found that some important intuitive concepts which proved to be useful in magnetism of $3d$ metals, such as the relationship between magnetic moments and coordination numbers, are not applicable to Rh clusters (and surfaces alike). Some other concepts, such as the Stoner model linking magnetic moments to DOS at the Fermi level, remain to be valid and useful.

II. COMPUTATIONAL METHOD

The calculations were performed in an *ab-initio* way within the spin density functional theory, relying on the local spin density approximation (LSDA) as parametrized by Vosko *et al.*²² The electronic structure is described fully relativistically by the corresponding Dirac equation. The computational approach is based on the multiple-scattering or Korringa-Kohn-Rostoker formalism²³ as implemented in the SPRKKR code.²⁴ The electronic structure problem is solved completely in real space. The potentials were treated within the atomic sphere approximation (ASA). For the angular momentum expansion of the Green function, a cutoff of $\ell_{\text{max}}=3$ was used. Only collinear magnetic structures were considered in this study.

The clusters were assumed to be spherical-like, containing 13–135 atoms, with fcc geometry as if cut from the bulk Rh crystal. They are centered either around an atom (13, 19, 43, 55, 79, 87, and 135 atoms) or around an interstitial empty site (14, 38, and 68 atoms). No structural relaxation was performed. The vacuum region was represented by empty sites located at lattice points. The network of these empty sites was built so that an empty site was included if it was a first- or second-nearest neighbor to any cluster atom.

We also performed some comparative calculations for isolated or free-standing (001), (110), and (111) monolayers and for the (001) crystal surface. These calculations were performed using supercell (multilayer) geometries. To simulate the crystal surface, we employed a slab consisting of 17 layers of Rh atoms. Successive Rh monolayers or slabs were separated by 13–20 Å of vacuum in the supercell. The integration over the \mathbf{k} -points was done on a regular mesh and for each of the systems the integration grid was chosen so that its density corresponds to (at least) 15625 \mathbf{k} -points in the full Brillouin zone of the

bulk Rh crystal. Otherwise the calculations were done as for the free clusters.

III. RESULTS

A. Magnetic moments

Local moments μ_{spin} , μ_{orb} and the ratio $\mu_{\text{orb}}/\mu_{\text{spin}}$ for clusters of 13–68 atoms are shown in Tab. I. Note that because of the presence of magnetization and of the SOC, atoms belonging to the same coordination shell need not be symmetry equivalent. Each value in Tab. I thus represents an average over all atoms located at the same distance R from the center of the cluster. The magnetization \mathbf{M} is parallel to the (001) direction of the parental fcc lattice.

No stable magnetic state was found for the 79-atoms and 87-atoms clusters. For the 135-atoms cluster a metastable magnetic state was identified (see also Sec. III C below), with sizable magnetic moments only at the last two coordination spheres: the average μ_{spin} (μ_{orb}) at the distance of 6.59 Å is 0.091 μ_B (0.017 μ_B) and average μ_{spin} (μ_{orb}) at the distance of 7.12 Å is 0.271 μ_B (0.025 μ_B).

Concerning the angular-momentum decomposition, the d component of μ_{spin} comprises 90–95% of its total value. For μ_{orb} the dominance of the d component is even more pronounced.

A better idea how the magnetic profiles look like may be obtained from representative graphs in Fig. 1. It appears from all the data that there is hardly any common trend in these profiles. This is in contrast to the case of $3d$ clusters where μ_{spin} and μ_{orb} generally increase towards the surface for all cluster sizes.¹⁴

B. Relation between local μ_{spin} and the coordination number

Our study covers a wide range of cluster sizes so it is possible to perform a systematic search for a relation between local moments and coordination numbers. Earlier studies failed to find a common trend like the one which had been identified before for the $3d$ clusters but in those studies always only a small range of cluster sizes was explored.^{4,6,18} We display in Fig. 2 local μ_{spin} as a function of the coordination number for magnetic clusters containing up to 135 atoms (including thus also the metastable 135-atoms cluster). It is evident from our data that no common rule concerning all atoms can be drawn for free Rh clusters.

C. Average magnetic moments and magnetization energies

A simple estimate of the strength of the magnetization can be obtained from average magnetic moments and from magnetization energies (differences of total energies per atom for a magnetic and a non-magnetic state). Furthermore, these quantities can be evaluated using fully-relativistic calculations and using the scalar-relativistic approximation,²⁵ providing thus an idea on the role of the SOC. We summarized these results in Tab. II. Note that μ_{orb} is zero in the scalar-relativistic approximation.

Average magnetic moments as well as magnetization energies generally decrease with cluster size, albeit non-monotonously. For the 68-atoms cluster the magnetic and non-magnetic states are practically degenerate, whereas for the 135-atoms cluster the ground state is non-magnetic. For a better understanding of the ΔE_{mag} values, recall that corresponding values for bulk $3d$ metals are 31.2 mRy, 29.8 mRy, and 3.6 mRy for Fe, Co, and Ni, respectively. Our results indicate that for large Rh clusters metastable isomers with different magnetic configurations should be expected, similarly as it was found for small Rh clusters.^{10–13}

One can see from Tab. II that the scalar-relativistic approximation overestimates μ_{spin} typically by about 10% (except for large clusters and/or small μ_{spin} where the relative difference is larger). In line with this, scalar-relativistic calculations yield larger magnetization energies.

D. Stoner criterion applied locally

When debating about magnetism of elements such as Ru, Rh, Pd, it is often argued that these metals could become magnetic in lower dimensions because then their density of states (DOS) at the Fermi energy $n(E_F)$ might increase due to band-narrowing, meaning that the Stoner criterion

$$I_s n(E_F) > 1 \quad , \quad (1)$$

with I_s being the Stoner integral, would be satisfied. It would be interesting to see to what extent does this criterion really govern magnetism of Rh. It would be instructive to look not only on the clusters but on surfaces and free-standing monolayers as well.

The Stoner exchange integral I_s is considered to be a quasi-atomic property, depending only very little on environmental effects such as bonding etc. We used the SPRKKR code to evaluate I_s for bulk Rh, for the (001) crystal surface and for free-standing (001), (110), and (111) monolayers.²⁶ The results are shown in Tab. III. One can see that indeed the exchange integral I_s varies only little from one Rh system to another.

Eq. (1) contains the DOS per spin channel $n(E_F)$ for the non-magnetic state. Strictly speaking, $n(E)$ is a

TABLE I. Local magnetic moments for clusters of different sizes, resolved according to the distance R from the cluster center. Each cluster is represented by one column. The first line for each R stands for μ_{spin} , the second for μ_{orb} and the third for the ratio $\mu_{\text{orb}}/\mu_{\text{spin}}$ (shown only if μ_{spin} is larger than $0.05 \mu_B$). The unit for R is \AA , the unit for μ_{spin} and μ_{orb} is μ_B .

R	Rh ₁₃	Rh ₁₄	Rh ₁₉	Rh ₃₈	Rh ₄₃	Rh ₅₅	Rh ₆₈
0.00	1.068		0.484		-0.007	0.011	
	-0.013		-0.170		-0.047	0.029	
	-0.012		-0.352		n/a	n/a	
1.90		1.193		0.457			0.01
		0.032		-0.046			0.01
		0.027		-0.101			n/a
2.69	1.452		0.864		0.099	0.296	
	0.118		0.138		-0.011	-0.013	
	0.081		0.161		-0.108	-0.044	
3.29		1.306		0.680			0.008
		0.234		-0.028			0.000
		0.179		-0.041			n/a
3.80			0.632		0.495	0.847	
			0.100		0.028	0.050	
			0.160		0.056	0.059	
4.25				0.761			0.004
				0.085			0.003
				0.112			n/a
4.65					0.190	0.718	
					0.017	0.060	
					0.087	0.084	
5.38						0.254	
						0.035	
						0.139	
5.71							0.134
							0.016
							0.062

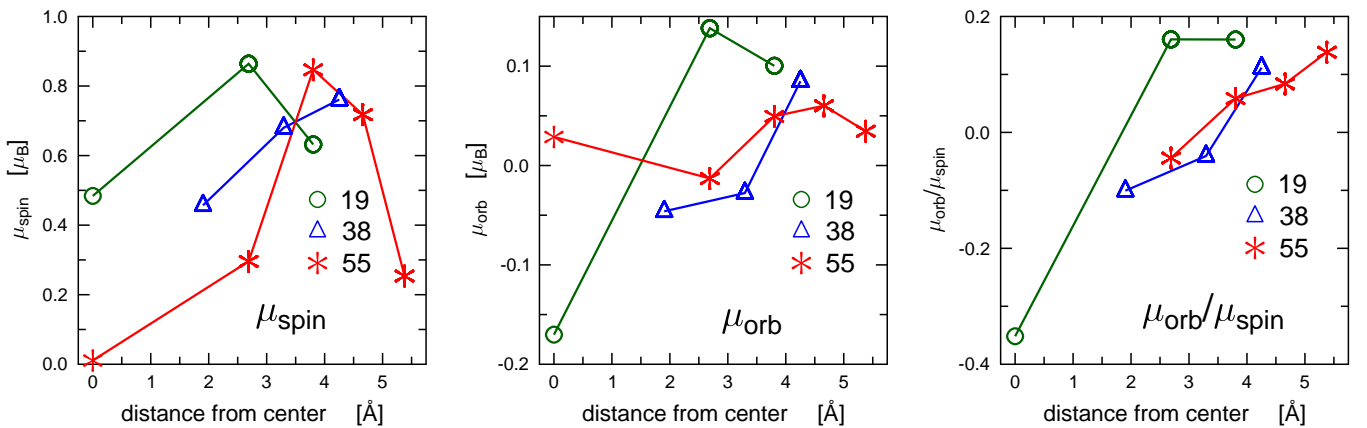


FIG. 1. (Color online) Magnetic profiles for clusters of 19, 38, and 55 atoms. Left and middle panels show μ_{spin} and μ_{orb} averaged over all atoms at given distance from the center. The right panel shows corresponding ratios μ_{orb} and μ_{spin} (the data point at $R=0$ for the 55-atoms cluster was omitted because the corresponding μ_{spin} is very small).

smooth function of E only if the energy levels form a continuous spectrum, which is the case for infinite solids but not for finite clusters, where the DOS is a sum of δ -functions, $n(E) = \sum_j \delta(E - E_j)$. However, for already relatively small clusters of 10–20 atoms one approaches

a quasicontinuum regime, with an energy level distribution that resembles that of a bulk crystal.^{27,28} One can construct an approximate DOS by broadening the energy levels by a Gaussian^{27,28} or Lorentzian.²⁹ In our Green function formalism the same is achieved by adding to E a

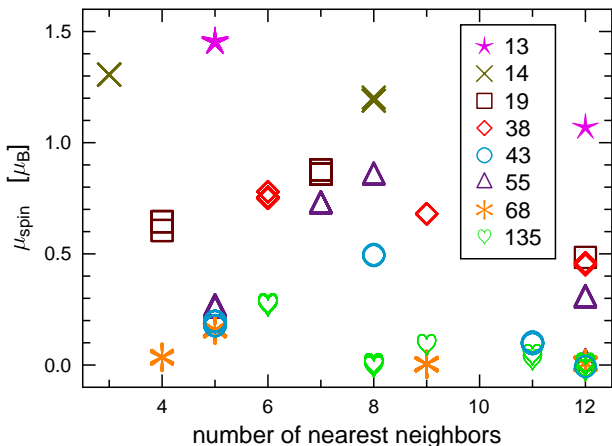


FIG. 2. (Color online) Local μ_{spin} as a function of the coordination number for atoms in clusters of 13–135 atoms.

TABLE II. Average magnetic moments in μ_B and magnetization energies per atom in mRy for clusters of 13–135 atoms. Apart from fully-relativistic results we display also μ_{spin} and ΔE_{mag} obtained via scalar-relativistic calculations.

N	μ_{spin}	μ_{spin} scalar	μ_{orb}	ΔE_{mag}	ΔE_{mag} scalar
13	1.423	1.604	0.108	-11.74	-13.82
14	1.258	1.433	0.147	-2.88	-3.55
19	0.771	0.823	0.110	-2.34	-2.63
38	0.696	0.785	0.040	-0.61	-1.47
43	0.202	0.254	0.009	-0.15	-0.22
55	0.526	0.563	0.037	-0.66	-1.15
68	0.062	0.088	0.009	0.00	-0.06
135	0.107	0.216	0.007	0.01	0.12

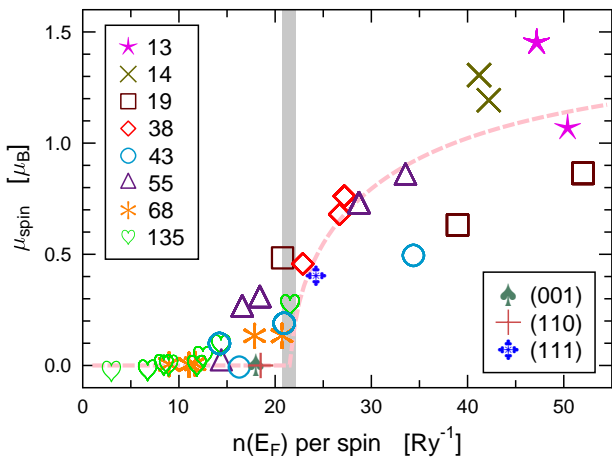


FIG. 3. (Color online) Dependence of μ_{spin} on the local density of states $n(E_F)$ calculated for non-magnetic clusters. Corresponding data for free-standing monolayers are included as well. The vertical band highlights the critical value of $n(E_F)$ when the Stoner product $I_s n(E_F)$ becomes larger than one. The dashed line is a fit to the Stoner model in Eq. (2).

TABLE III. Stoner exchange integral I_s , DOS per spin channel at E_F in a non-magnetic state, Stoner product $I_s n(E_F)$ and magnetic moment for two-dimensional Rh systems.

system	I_s mRy	$n(E_F)$ Ry^{-1}	$I_s n(E_F)$	μ_{spin} μ_B
(100) monolayer	46.7	18.0	0.84	0.00
(110) monolayer	45.5	18.5	0.84	0.00
(111) monolayer	45.2	24.3	1.10	0.40
(100) surface	44.9	11.4	0.51	0.00
bulk	48.2	9.9	0.48	0.00

small imaginary part $\text{Im}E$, which is equivalent to broadening the levels by a Lorentzian with full width at half maximum of $2\text{Im}E$. In this way we can evaluate $n(E_F)$ for every atom in all the clusters we investigate. If we choose $\text{Im}E=3$ mRy, we obtain a graph for the dependence of the local μ_{spin} on the corresponding $n(E_F)$ shown in Fig. 3. The thick vertical gray line in Fig. 3 highlights the “critical DOS” which separates magnetic systems from non-magnetic systems according to Eq. (1).

One can see that the Stoner criterion (1) can be used with a good accuracy to predict whether a particular Rh atom will be magnetic or not. To be more precise, it follows from Fig. 3 that the criterion (1) is a bit too strict — one can get magnetism also for atoms where $n(E_F)$ is by 10–20% lower than the critical value. If the Stoner model for the dependence of μ_{spin} on $n(E_F)$ is adopted,³⁰

$$\mu_{\text{spin}} \sim \sqrt{1 - \frac{1}{I_s n(E_F)}} \quad \Leftrightarrow \quad n(E_F) > \frac{1}{I_s}, \quad (2)$$

$$\mu_{\text{spin}} = 0 \quad \Leftrightarrow \quad n(E_F) < \frac{1}{I_s}$$

(see the Fig. 3), the best fit is obtained for $I_s=46.1$ mRy, in very good agreement with the directly computed values shown in Tab. III. So it turns out that the Stoner model can serve as a guide to Rh magnetism, even concerning its local aspects. We verified that this does not depend on the particular value of the DOS broadening we used. In fact graphs similar to Fig. 3 can be obtained if $\text{Im}E$ is varied within a reasonable interval 1–10 mRy.

Corresponding data for bulk and two-dimensional Rh systems are shown in Tab. III. The only two-dimensional system which is magnetic is the (111) free-standing monolayer and it is also the only one which satisfies the criterion given by Eq. (1). We included these data in Fig. 3 to demonstrate that they follow the same trend as the data for clusters.

E. Anisotropy of μ_{orb} and T_z

The relatively strong SOC for Rh implies that μ_{orb} could play a more important role than in the case of 3d clusters. Its effects are also accessible to experiment via XMCD; partially conflicting result were obtained in

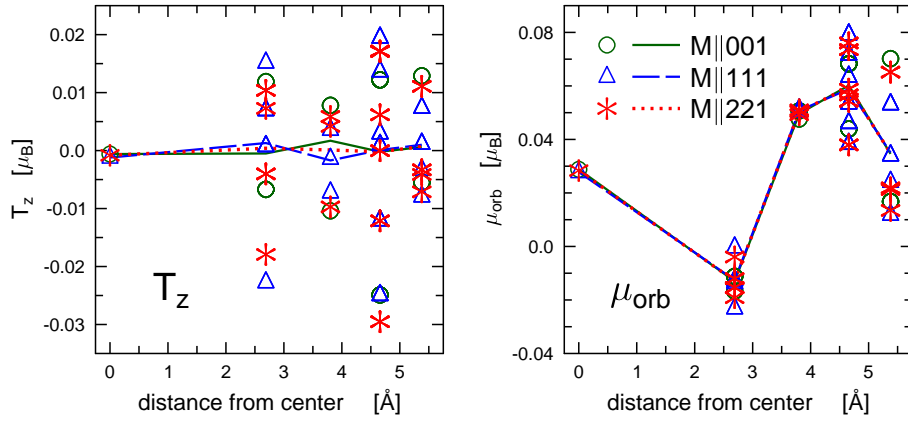


FIG. 4. (Color online) Dependence of the d component of the T_z term and of μ_{orb} on the magnetization direction for the 55-atoms cluster. Markers show values associated with individual atoms, lines show values averaged over all atoms at the same distance. The orientation of the magnetization \mathbf{M} with respect to the underlying fcc lattice is specified in the legend.

this respect.^{2,3} Linked to the use of the XMCD is also the magnetic dipole term because the XMCD sum rules deal not with μ_{spin} alone but only with a combination $\mu_{spin} + 7T_z$, where T_z is the expectation value of the intra-atomic dipole operator for the valence d electrons (assuming that the z axis is chosen parallel to \mathbf{M}). Both μ_{orb} and T_z depend on the magnetization direction.^{31–33} This dependence was studied for $3d$ free clusters¹⁴ and adatoms³⁴ in the past. The T_z term can significantly affect the perceived dependence of μ_{spin} on the cluster size³⁵ and it was suggested that this might occur also for $4d$ clusters.²¹

We calculated μ_{orb} and T_z for several magnetization directions, for all the cluster sizes we explore here. As a representative example we select the 55-atoms cluster with \mathbf{M} parallel to the [001], [111], and [221] crystallographic directions. The results are shown in Fig. 4. One notices immediately the effect of the decrease of the symmetry due to the magnetization and the SOC: there is a significant spread in the T_z and μ_{orb} values for atoms which are at the same distance from the center. There is also a significant dependence on the direction of \mathbf{M} for T_z and μ_{orb} of the individual atoms.

When looking at the T_z term, we can see that as concerns individual atoms, T_z could indeed be the cause of a significant difference between μ_{spin} and $\mu_{spin} + 7T_z$; the magnitude of $7T_z$ is sometimes comparable to the corresponding μ_{spin} for the Rh_{55} cluster (see also Tab. I). However, the averaged or “cumulative” values of T_z are very small, as evidenced by the lines in the left panel of Fig. 4. This is apparently linked to the fact that our clusters are spherical-like and therefore averaging over atoms for a fixed magnetization direction is approximately equivalent to averaging over magnetization directions for a fixed atom. Such an averaging should yield a small value for T_z due to the approximate relation $T_x + T_y + T_z = 0$ (valid exactly in the absence of the SOC).³¹ Therefore, as the measured XMCD always reflects all atoms in the cluster,

it seems that the T_z term cannot affect the interpretation of XMCD experiments for free Rh clusters. At least — not as long as they remain approximately spherical.

Concerning the orbital moments (right panel of Fig. 4), again we can see a significant anisotropy when focusing on individual atoms but hardly any anisotropy when focusing on the average values (similarly as for free Fe clusters).¹⁴ This apparently reflects the fact that the geometry of the clusters is cubic.

IV. DISCUSSION

Our goal was to search for common trends governing magnetism of Rh clusters, especially those with more than about 20 atoms. We found that there is no systematic link between magnetic moments and coordination numbers. On the other hand, systematic trends can be identified in the dependence of μ_{spin} on $n(E_F)$. Metastable magnetic states exist for large clusters. The influence of the SOC on magnetism of Rh is not negligible but not crucial either.

The lack of a systematic relation between local magnetic moments and coordination numbers is perhaps the most striking feature of magnetism of Rh in comparison with magnetism of $3d$ metals. It means that intuitive arguments which are routinely used when analyzing magnetism of $3d$ metals cannot be applied. This can be illustrated by the case of free-standing Rh monolayers of different crystallographic types (see Tab. III) where the only one which is magnetic is the one with the *largest* coordination number. It is interesting to note that another kind of unusual trend in Rh magnetism was observed before, namely, the increase of magnetic moments of Rh adatoms on Ag(001) with decreasing interatomic distance.³⁶ Unusual magnetic behaviour of Rh can thus be expected in a variety of environments.

We conjecture that the “anomalous” behavior of Rh observed here is linked to the fact that $4d$ electrons are less localized than $3d$ electrons and thus the dominance of the nearest-neighbors influence over the influence of more distant neighbors is much smaller for the $4d$ metals than for the $3d$ metals. To be quantitative, for metallic Co, which is a $3d$ analogue of Rh, the center of mass of the valence d wave function defined as $r_{3d} = |\langle \psi_{3d} | r | \psi_{3d} \rangle|$ is at about 0.52 \AA , which presents 21% of the bulk interatomic distance. (A $\psi_{3d}(\mathbf{r})$ wave function obtained for a representative energy corresponding to the highest majority-spin states DOS was used.) This should be compared to the d wave function for metallic Rh for which one gets $r_{4d} \approx 0.78 \text{ \AA}$, which presents 31% of the bulk interatomic distance. Our results also complement arguments of Mavropoulos *et al.*¹⁵ concerning magnetic moments of supported $3d$ and $4d$ clusters.

The Stoner model appears well-suited for describing magnetism of $4d$ metals. It proves to be useful as a criterion for the onset of magnetism, as it was demonstrated recently for Rh monolayers on noble metals surfaces.³⁷ However, it serves also as a guide for the dependence of the magnitude of local magnetic moments on the DOS at the Fermi level. Here we would like to mention that a relationship between local μ_{spin} and $n(E_F)$ was observed also for thin Pd slabs,³⁸ again underlining the relevance of the Stoner model for magnetism of $4d$ systems. This supports the argumentation of Barthem *et al.*³ that in large Rh clusters some atoms may be magnetic and others non-magnetic because $n(E_F)$ may differ a lot from one atom to another.

Even though the SOC does not play a prominent role in Rh magnetism, there may be situations where it is quite important. This is illustrated by the case of the central atom of the Rh₁₉ cluster where μ_{orb} reaches 35% of μ_{spin} and is oriented *antiparallel* to μ_{spin} (see Tab. I). Antiparallel orientation of μ_{orb} can be observed also for the Rh₃₈ cluster. This finding is interesting because an antiparallel orientation of μ_{orb} for some atoms might explain why only very small averaged orbital moments were found for embedded Rh clusters via the XMCD measurements of Barthem *et al.*³

A large antiparallel μ_{orb} for some Rh clusters was obtained by our fully-relativistic *ab-initio* calculations but not by earlier model d -band TB Hamiltonian calculations where the SOC was added within the second variation approach.¹⁹ A detailed comparison between our results and the model Hamiltonian results is presented in Tab. IV for Rh₁₃ and Rh₁₉ clusters (moments for the same geometries are shown). One can see that there is a general agreement between both calculations but differences occur for some atoms.

All our calculations were done for bulk-like, i.e., unrelaxed geometries. Changing the interatomic distances would of course affect the calculated μ_{spin} and μ_{orb} . *Ab-initio* calculations for clusters of 2–19 atoms found that bond-length contraction of 4–8 % may lead to large changes of magnetic moments, in particular for a 4-

TABLE IV. Magnetic moments in μ_B from our fully-relativistic *ab-initio* calculations compared to results obtained via a model d -band TB Hamiltonian with an additional SOC term.¹⁹ Results for the Rh₁₃ and Rh₁₉ clusters are resolved according to distances of atoms from the center of the cluster, as indicated by the indices in the parantheses in the first column. Two different values of μ_{orb} are often present because magnetization together with the SOC decreases the symmetry in a fully relativistic treatment.

shell		this work	model Hamiltonian ¹⁹
Rh ₁₃ (1)	μ_{spin}	1.07	1.19
Rh ₁₃ (1)	μ_{orb}	-0.01	-0.01
Rh ₁₃ (2)	μ_{spin}	1.45	1.62
Rh ₁₃ (2)	μ_{orb}	0.10, 0.15	0.30
Rh ₁₉ (1)	μ_{spin}	0.48	1.21
Rh ₁₉ (1)	μ_{orb}	-0.17	0.13
Rh ₁₉ (2)	μ_{spin}	0.86	1.11
Rh ₁₉ (2)	μ_{orb}	0.17, 0.07	0.14
Rh ₁₉ (3)	μ_{spin}	0.63	0.70
Rh ₁₉ (3)	μ_{orb}	0.14, 0.08	0.16

atoms cluster and a 10-atoms cluster.¹⁰ However, the bond length changes are less important for large clusters — in fact, model Hamiltonian calculations suggest a bond-length contraction of about 4 % for clusters of 8–13 atoms but only 1–3 % for clusters of 55 and 147 atoms.³⁹ Another study based on semi-empirical potential and model *spd* TB Hamiltonians found that the average nearest-neighbor distance is close to the bulk-like distance for clusters of more than about 20 atoms.¹⁸ Let us also mention a model Hamiltonian study which found that using equilibrium bond lengths instead of bulk bond lengths changes μ_{spin} and μ_{orb} by about 50 % for a cluster of 13 atoms while for clusters of 19 and 27 atoms the bond relaxation decreases μ_{spin} only by about 10% and μ_{orb} by about 20%.¹⁹ The fcc growth mode adopted here is plausible in the light of the *ab initio* study of Futschek *et al.*¹³ who found that clusters of more than about ten atoms adopt ground state geometries that can be considered as fragments of the fcc crystal structure. We conclude that while small clusters of less than ~ 10 atoms are quite sensitive to structural relaxation, results for large Rh clusters are not so dependent on whether the structural relaxation has been performed or not.

When compared with experiment on free Rh clusters,¹ our calculation gives higher average magnetic moments in the 13–55 atoms size range. A d band TB model Hamiltonian study of fcc clusters⁹ gave similar values as our study while an *ab initio* pseudopotential-based calculations of icosahedral clusters¹² led to smaller values, in a better agreement with the experiment. However, one should be cautious about drawing conclusions, say, about preference of the icosahedral geometry over the fcc geometry just from this: in all the theoretical studies, only few cluster sizes were considered beyond the 20-atoms limit and the dependence of the average magnetic moment on the

cluster size displays a quasi-oscillatory behavior, so one cannot be sure how representative the results are. One should also take into account that in the case of small clusters, where more theoretical studies we performed, the results often differ substantially from one study to another.^{4-8,12,13} It turns out that accurate calculations which could be directly compared to experiment are very difficult to perform because the systems are quite complex and there are many factors to control. Therefore, it is useful to perform a study like the current one which focuses on the analysis of general trends and rules which the Rh cluster should obey, to improve our intuitive understanding.

V. CONCLUSIONS

Some important intuitive concepts which proved to be useful in interpreting the magnetism of $3d$ metals are not applicable to magnetism of $4d$ systems such as Rh clusters. In particular there is no systematic relation between local magnetic moments and coordination numbers. On the other hand, the Stoner model describes even local

aspect of Rh magnetism quite well; atoms for which the DOS in the non-magnetic state $n(E_F)$ is more than 20 states per spin per Ry will be magnetic.

Fully-relativistic calculations indicate that there can be large μ_{orb} antiparallel to μ_{spin} for some atoms. The intra-atomic T_z term can be quite large at certain sites but as a whole it is unlikely to affect the interpretation of XMCD experiments based on the sum rules. For clusters in the ~ 100 atoms size range it is likely that there will be metastable magnetic configurations, with excitation energies less than 0.1 mRy per atom.

ACKNOWLEDGMENTS

Financial support by the Grant Agency of the Czech Republic within the project 108/11/0853 and by the Deutsche Forschungsgemeinschaft within the project SFB 689 is gratefully acknowledged. J.M. also acknowledges support by the CENTEM project CZ.1.05/2.1.00/03.0088, co-funded by the ERDF as part of the Ministry of Education, Youth and Sports OP RDI programme.

* sivr@fzu.cz; <http://www.fzu.cz/~sivr>

- ¹ A. J. Cox, J. G. Louderback, S. E. Apsel, and L. A. Bloomfield, *Phys. Rev. B* **49**, 12295 (1994).
- ² V. Sessi, K. Kuhnke, J. Zhang, J. Honolka, K. Kern, C. Tieg, O. Šipr, J. Minár, and H. Ebert, *Phys. Rev. B* **82**, 184413 (2010).
- ³ V. M. T. S. Barthem, A. Rogalev, F. Wilhelm, M. M. Sant'Anna, S. L. A. Mello, Y. Zhang, P. Bayle-Guillemaud, and D. Givord, *Phys. Rev. Lett.* **109**, 197204 (2012).
- ⁴ Y.-C. Bae, H. Osanai, V. Kumar, and Y. Kawazoe, *Phys. Rev. B* **70**, 195413 (2004).
- ⁵ C. M. Chang and M. Y. Chou, *Phys. Rev. Lett.* **93**, 133401 (2004).
- ⁶ F. Aguilera-Granja, J. M. Montejano-Carrizalez, and R. A. Guirado-López, *Phys. Rev. B* **73**, 115422 (2006).
- ⁷ M. R. Beltrán, F. Buendía Zamudio, V. Chauhan, P. Sen, H. Wang, Y. J. Ko, and K. Bowen, *Eur. Phys. J. D* **67**, 1 (2013).
- ⁸ F. Aguilera-Granja, L. C. Balbás, and A. Vega, *J. Phys. Chem. A* **113**, 13483 (2009).
- ⁹ R. Guirado-López, M. C. Desjonquères, and D. Spanjaard, *Phys. Rev. B* **62**, 13188 (2000).
- ¹⁰ Y. Jinlong, F. Toigo, and W. Kélin, *Phys. Rev. B* **50**, 7915 (1994).
- ¹¹ K. Lee, *Z. Phys. D* **40**, 164 (1997).
- ¹² V. Kumar and Y. Kawazoe, *Eur. Phys. J. D* **24**, 81 (2003).
- ¹³ T. Futschek, M. Marsman, and J. Hafner, *J. Phys.: Condens. Matter* **17**, 5927 (2005).
- ¹⁴ O. Šipr, M. Košuth, and H. Ebert, *Phys. Rev. B* **70**, 174423 (2004).
- ¹⁵ P. Mavropoulos, S. Lounis, R. Zeller, P. H. Dederichs, and S. Blügel, *Appl. Physics A* **82**, 103 (2006).
- ¹⁶ O. Šipr, S. Bornemann, J. Minár, S. Polesya, V. Popescu, A. Šimůnek, and H. Ebert, *J. Phys.: Condens. Matter* **19**,

096203 (2007).

- ¹⁷ S. Bornemann, O. Šipr, S. Mankovsky, S. Polesya, J. B. Staunton, W. Wurth, H. Ebert, and J. Minár, *Phys. Rev. B* **86**, 104436 (2012).
- ¹⁸ F. Aguilera-Granja, J. L. Rodríguez-López, K. Michaelian, E. O. Berlanga-Ramírez, and A. Vega, *Phys. Rev. B* **66**, 224410 (2002).
- ¹⁹ R. Guirado-Lopez, P. Villasenor-Gonzalez, J. Dorantes-Davila, and G. M. Pastor, *J. Appl. Phys.* **87**, 4906 (2000).
- ²⁰ R. A. Guirado-López, J. Dorantes-Dávila, and G. M. Pastor, *Phys. Rev. Lett.* **90**, 226402 (2003).
- ²¹ H. K. Yuan, H. Chen, A. L. Kuang, B. Wu, and J. Z. Wang, *J. Phys. Chem. A* **116**, 11673 (2012).
- ²² S. H. Vosko, L. Wilk, and M. Nusair, *Can. J. Phys.* **58**, 1200 (1980).
- ²³ H. Ebert, D. Ködderitzsch, and J. Minár, *Rep. Prog. Phys.* **74**, 096501 (2011).
- ²⁴ H. Ebert, *The Munich SPR-KKR package, version 3.6*, <http://olymp.cup.uni-muenchen.de> (2005).
- ²⁵ D. D. Koelling and B. N. Harmon, *J. Phys. C: Solid State Phys.* **10**, 3107 (1977).
- ²⁶ O. Gunnarsson, *J. Phys. F: Met. Phys.* **6**, 587 (1976).
- ²⁷ C. Y. Yang, K. H. Johnson, D. R. Salahub, J. Kaspar, and R. P. Messmer, *Phys. Rev. B* **24**, 5673 (1981).
- ²⁸ K. Lee, J. Callaway, and S. Dhar, *Phys. Rev. B* **34**, 1724 (1984).
- ²⁹ F. Liu, S. N. Khanna, and P. Jena, *Phys. Rev. B* **43**, 8179 (1991).
- ³⁰ J. Sólyom, *Fundamentals of the Physics of Solids: Volume 3 - Normal, Broken-Symmetry, and Correlated Systems* (Springer, Berlin, 2010).
- ³¹ J. Stöhr and H. König, *Phys. Rev. Lett.* **75**, 3748 (1995).
- ³² H. A. Dürr and G. van der Laan, *Phys. Rev. B* **54**, R760 (1996).

- ³³ J. Stöhr, *J. Magn. Magn. Materials* **200**, 470 (1999).
- ³⁴ O. Šipr, S. Bornemann, H. Ebert, S. Mankovsky, J. Vackář, and J. Minár, *Phys. Rev. B* **88**, 064411 (2013).
- ³⁵ O. Šipr, J. Minár, and H. Ebert, *Europhys. Lett.* **87**, 67007 (2009).
- ³⁶ V. S. Stepanyuk, W. Hergert, P. Rennert, J. Izquierdo, A. Vega, and L. C. Balbás, *Phys. Rev. B* **57**, R14020 (1998).
- ³⁷ L. Garcia-Cruz and R. Baquero, *Rev. Mex. Fis.* **49**, 317 (2003).
- ³⁸ S. C. Hong, J. I. Lee, and R. Wu, *J. Magn. Magn. Materials* **310**, 2262 (2007).
- ³⁹ C. Barreteau, R. Guirado-López, D. Spanjaard, M. C. Desjonquères, and A. M. Oleś, *Phys. Rev. B* **61**, 7781 (2000).